13

Continuity equation and the Fokker–Planck approach

In the previous chapter, the notion of a homogeneous population of neurons was introduced. Neurons within the population can be independent, fully connected, or randomly connected, but they should all have identical, or at least similar, parameters and all neurons should receive similar input. For such a homogeneous population of neurons, it is possible to predict the population activity in the stationary state of asynchronous firing (Section 12.4). While the arguments we made in the previous chapter are general and do not rely on any specific neuron model, they are unfortunately restricted to the stationary state.

In a realistic situation, neurons in the brain receive time-dependent input. Humans change their direction of gaze spontaneously two or three times per second. After each gaze change, a new image impinges on the retina and is transmitted to the visual cortex. Auditory stimuli such as music or traffic noise have a rich intrinsic temporal structure. If humans explore the texture of a surface which by itself is static, they move their fingers so as to actively create temporal structure in the touch perception. If we think back to our last holiday, we recall sequences of events rather than static memory items. When we type a message on a keyboard, we move our fingers in a rapid pattern. In *none* of these situations, is *stationary* brain activity a likely candidate to represent our thoughts and perceptions. Indeed, EEG (electroencephalography) recordings from the surface of the human scalp, as well as multi-unit activity recorded from the cortex of animals, indicate that the activity of the brain exhibits a rich temporal structure.

In this chapter, we present a formulation of population activity equations that can account for the temporal aspects of population dynamics. It is based on the notion of membrane potential densities for which a continuity equation is derived (Section 13.1). In order to illustrate the approach, we consider a population of neurons receiving stochastically arriving spikes (Sections 13.2 and 13.3). For an explicit solution of the equations, we first focus on coupled populations of leaky integrate-and-fire neurons (Sections 13.4), but the mathematical approach can be generalized to arbitrary nonlinear integrate-and-fire neurons (Section 13.5) and generalized integrate-and-fire neurons with adaptation (Section 13.6).

Before we turn to neurons with adaptation, we focus on one-dimensional, but potentially nonlinear integrate-and-fire neurons. Knowledge of the momentary membrane potential

and the input is sufficient to predict the future evolution of a single integrate-and-fire neuron. In a large population of neurons, the momentary state of the population as a whole can therefore be characterized by the momentary distribution of membrane potentials. The evolution of this distribution over time is summarized by the continuity equation which is introduced now.

13.1 Continuity equation

In a population of neurons, each neuron may be in a different internal state. In this section we derive partial differential equations that describe how the distribution of internal states evolves as a function of time. We start in Section 13.1.1 with a population of integrate-and-fire neurons. Since the state of an integrate-and-fire neuron is characterized by its membrane potential, we describe the dynamics of the population as the evolution of membrane potential densities.

The population activity, $A(t)$, was introduced in Chapter 7 as the fraction of neurons that fire at time t in a finite population. In this chapter and the next, the population activity is the expected population activity $A(t) \equiv \langle A(t) \rangle$. Since A(t) is self-averaging, it can also be said that we consider the limit of large populations. The finite-size effects will be discussed in Section 14.6.

The formulation of the dynamics of a population of integrate-and-fire neurons on the level of membrane potential densities has been developed by Abbott and van Vreeswijk (1993), Brunel and Hakim (1999), Fusi and Mattia (1999), Nykamp and Tranchina (2000), Brunel (2000), and Omurtag *et al*. (2000). The closely related formulation in terms of refractory densities has been studied by Wilson and Cowan (1972), Gerstner and van Hemmen (1992), Bauer and Pawelzik (1993), and Gerstner (2000). Generalized density equations have been discussed by Knight (2000) and Fourcaud and Brunel (2002).

13.1.1 Distribution of membrane potentials

We study a homogeneous population of integrate-and-fire neurons. The internal state of a neuron i is determined by its membrane potential which changes according to

$$\tau_m \frac{\mathrm{d}}{\mathrm{d}t} u_i = f(u_i) + R I_i(t) \quad \text{for } u_i < \theta_{\text{reset}} \,. \tag{13.1}$$

Here R is the input resistance, $\tau_m = RC$ the membrane time constant, and $I_i(t)$ the total input (external driving current and synaptic input). If $u_i \geq \theta_{\text{reset}}$ the membrane potential is reset to $u_i = u_r < \theta_{\text{reset}}$. Here $f(u_i)$ is an arbitrary function of u; see Eq. (5.2). For $f(u_i) = -(u_i - u_{\text{rest}})$ the equation reduces to the standard leaky integrate-and-fire model. For the moment we keep the treatment general and restrict it to the leaky integrate-and-fire model only later.

In a population of N integrate-and-fire neurons, we may ask how many of the neurons

https://doi.org/10.1017/CBO9781107447615.016 Published online by Cambridge University Press

have at time t a given membrane potential. As $N \to \infty$ the fraction of neurons i with membrane potential $u_0 < u_i(t) \le u_0 + \Delta u$ is

$$\lim_{N\to\infty} \left\{ \frac{\text{neurons with } u_0 < u_i(t) \le u_0 + \Delta u}{N} \right\} = \int_{u_0}^{u_0+\Delta u} p(u,t)\,\mathrm{d}u\,, \tag{13.2}$$

where $p(u,t)$ is the *membrane potential density*; see Chapter 8. The integral over this density remains constant over time, i.e.,

$$\int_{-\infty}^{\theta_{\text{reset}}} p(u,t)\,\mathrm{d}u = 1\,. \tag{13.3}$$

The normalization to unity expresses the fact that all neurons have a membrane potential below or equal to the threshold.

The aim of this section is to describe the evolution of the density $p(u,t)$ as a function of time. As we shall see, the equation that describes the dynamics of $p(u,t)$ is nearly identical to that of a single integrate-and-fire neuron with diffusive noise; see Eqs. (8.40) and (8.41).

13.1.2 Flux and continuity equation

Let us consider the portion of neurons with a membrane potential between u_0 and u_1,

$$\frac{n(u_0;u_1)}{N} = \int_{u_0}^{u_1} p(u',t)\,\mathrm{d}u'\,. \tag{13.4}$$

The fraction of neurons with $u_0 < u < u_1$ increases if neurons enter from below through the boundary u_0 or from above through the boundary u_1; see Fig. 13.1. Since there are many neurons in the population, we expect that in each short time interval Δt, many trajectories cross one of the boundaries. The *flux* $J(u,t)$ is the net fraction of trajectories per unit time that crosses the value u. A positive flux $J(u,t) > 0$ is defined as a flux toward increasing values of u. In other words, in a finite population of N neurons, the quantity $NJ(u_0,t)\Delta t$ describes the number of trajectories that in the interval Δt cross the boundary u_0 from below, minus the number of trajectories crossing u_0 from above. Note that u_0 here is an arbitrary value that we chose as the lower bound of the integral in Eq. (13.4) and as such has no physical meaning for the neuron model.

Since trajectories cannot simply end, a change in the number $n(u_0;u_1)$ of trajectories in the interval $u_0 < u < u_1$ can be traced back to the flux of trajectories in and out of that interval. We therefore have the conservation law

$$\frac{\partial}{\partial t}\int_{u_0}^{u_1} p(u',t)\,\mathrm{d}u' = J(u_0,t) - J(u_1,t). \tag{13.5}$$

Taking the derivative with respect to the upper boundary u_1 and changing the name of the variable from u_1 to u yields the continuity equation,

$$\frac{\partial}{\partial t}p(u,t) = -\frac{\partial}{\partial u}J(u,t) \quad \text{for } u \neq u_r \text{ and } u \neq \theta_{\text{reset}}\,, \tag{13.6}$$

https://doi.org/10.1017/CBO9781107447615.016 Published online by Cambridge University Press

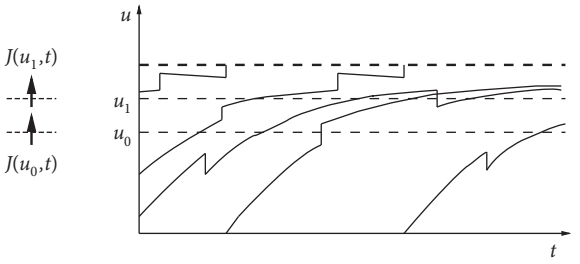

Fig. 13.1 The number of trajectories in the interval $[u_0, u_1]$ changes if one of the trajectories crosses the boundary u_0 or u_1. For a large number of neurons this fact is described by the continuity equation; see Eq. (13.6). Schematic figure where only three trajectories are shown.

which expresses the conservation of the number of trajectories. In integrate-and-fire models, however, there are two special voltage values, u_r and θ_{reset}, where the number of trajectories is *not* conserved, because of the fire-and-reset mechanism.

Since neurons that have fired start a new trajectory at u_r, we have a "source of new trajectories" at $u = u_r$, i.e., new trajectories appear in the interval $[u_r - \varepsilon, u_r + \varepsilon]$ that have not entered the interval through one of the borders. Adding a term $A(t)\,\delta(u - u_r)$ on the right-hand side of (13.6) accounts for this source of trajectories. The trajectories that appear at u_r disappear at θ_{reset}, so that we have

$$\frac{\partial}{\partial t}p(u,t) = -\frac{\partial}{\partial u}J(u,t) + A(t)\,\delta(u - u_r) - A(t)\,\delta(u - \theta_{\text{reset}})\,. \tag{13.7}$$

The density $p(u,t)$ vanishes for all values $u > \theta_{\text{reset}}$.

The population activity $A(t)$ is, by definition, the fraction of neurons that fire, i.e., those that pass through the threshold. Therefore we find

$$A(t) = J(\theta_{\text{reset}}, t)\,. \tag{13.8}$$

Equations (13.7) and (13.8) describe the evolution of the the membrane potential densities and the resulting population activity as a function of time. We now specify the neuron model so as to have an explicit expression for the flux.

13.2 Stochastic spike arrival

We consider the flux $J(u,t)$ in a homogeneous population of integrate-and-fire neurons with voltage equation (13.1). We assume that all neurons in the population receive the same driving current I^{ext}. In addition each neuron receives independent background input in the form of stochastic spike arrival. We allow for different types of synapses. An input spike at a synapse of type k causes a jump of the membrane potential by an amount w_k. For example, $k = 1$ could refer to weak excitatory synapses with jump size $w_1 > 0$; $k = 2$ to strong excitatory synapses $w_2 > w_1$; and $k = 3$ to inhibitory synapses with $w_3 < 0$. The effective spike arrival rate (summed over all synapses of the same type k) is denoted

https://doi.org/10.1017/CBO9781107447615.016 Published online by Cambridge University Press

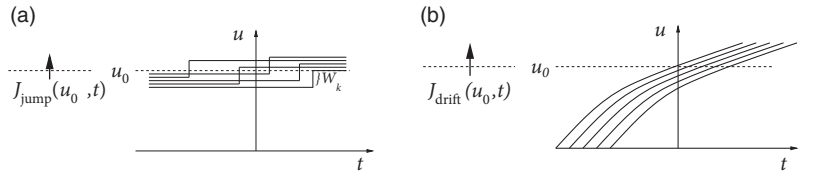

Fig. 13.2 (a) All trajectory that are less than w_k below u_0 cross u_0 upon spike arrival. (b) The drift $J_{\text{drift}}(u_0,t)$ depends on the density of the trajectories and on the slope with which the trajectories cross the boundary u_0.

as ν_k. While the mean spike arrival rates $\nu_k(t)$ are identical for all neurons, we assume that the actual input spike trains at different neurons and different synapses are independent. In a simulation, spike arrival at different neurons is generated by independent Poisson processes with a common spike arrival rate $\nu_k(t)$ for synapse type k.

Whereas spike arrivals cause a jump of the membrane potential, a finite input current $I^{\text{ext}}(t)$ generates a smooth drift of the membrane potential trajectories. In such a network, the flux $J(u,t)$ across a reference potential u_0 can therefore be generated in two different ways: through a "jump" or a "drift" of trajectories. We separate the two contributions to the flux into J_{jump} and J_{drift}

$$J(u_0,t) = J_{\text{drift}}(u_0,t) + J_{\text{jump}}(u_0,t)\,, \tag{13.9}$$

and treat each of these in turn.

13.2.1 Jumps of membrane potential due to stochastic spike arrival

To evaluate J_{jump}, let us consider an excitatory input $w_k > 0$. All neurons that have a membrane potential u_i with $u_0 - w_k < u_i \leq u_0$ will jump across the reference potential u_0 upon spike arrival at a synapse of type k; see Fig. 13.2a. Since at each neuron spikes arrive stochastically, we cannot predict with certainty whether a single neuron receives a spike around time t or not. But because the Poisson rate ν_k of spike arrival at synapses of type k is the same for each neuron, while the actual spike trains are independent for different neurons, the total (expected) flux, or probability current, caused by input spikes at all synapses can be calculated as

$$J_{\text{jump}}(u_0,t) = \sum_k \nu_k \int_{u_0-w_k}^{u_0} p(u,t)\,\mathrm{d}u\,. \tag{13.10}$$

If the number of neurons is large, the actual flux is very close to the expected flux given in Eq. (13.10).

https://doi.org/10.1017/CBO9781107447615.016 Published online by Cambridge University Press

13.2.2 Drift of membrane potential

The drift flux $J_{\rm drift}(u_0,t)$ through the reference potential u_0 is given by the density $p(u_0,t)$ at the potential u_0 times the momentary "velocity" $\mathrm{d}u/\mathrm{d}t$; see Fig. 13.2b. Therefore

$$J_{\rm drift}(u_0,t) = \left.\frac{\mathrm{d}u}{\mathrm{d}t}\right|_{u_0} p(u_0,t) = \frac{1}{\tau_m}\left[f(u_0) + RI^{\rm ext}(t)\right] p(u_0,t)\,, \tag{13.11}$$

where $f(u_0)$ is the nonlinearity of the the integrate-and-fire model in Eq. (13.1). Note that synaptic δ-current pulses cause a jump of the membrane potential and therefore contribute only to $J_{\rm jump}$ (see Section 13.2.1), but not to the drift flux considered here. Current pulses of finite duration, however, should be included in $I^{\rm ext}(t)$ in Eq. (13.11).

Example: Leaky integrate-and-fire neurons

With $f(u) = -(u - u_{\rm rest})$ we have for leaky integrate-and-fire neurons a drift-induced flux

$$J_{\rm drift}(u_0,t) = \frac{1}{\tau_m}\left[-u_0 + u_{\rm rest} + RI^{\rm ext}(t)\right] p(u_0,t)\,. \tag{13.12}$$

13.2.3 Population activity

A positive flux through the threshold $\theta_{\rm reset}$ yields the population activity $A(t)$. Since the flux has components from the drift and from the jumps, the total flux at the threshold is

$$A(t) = \frac{1}{\tau_m}\left[f(\theta_{\rm reset}) + RI^{\rm ext}(t)\right] p(\theta_{\rm reset},t) + \sum_k \nu_k \int_{\theta_{\rm reset}-w_k}^{\theta_{\rm reset}} p(u,t)\,\mathrm{d}u\,. \tag{13.13}$$

Since the probability density vanishes for $u > \theta_{\rm reset}$, the sum over the synapses k can be restricted to all *excitatory* synapses.

If we insert the explicit form of the flux that we derived in Eqs. (13.10) and (13.11) into the continuity equation (13.7), we arrive at the density equation for the membrane potential of integrate-and-fire neurons

$$\begin{aligned}\frac{\partial}{\partial t}p(u,t) = &-\frac{1}{\tau_m}\frac{\partial}{\partial u}\left\{\left[f(u) + RI^{\rm ext}(t)\right]\, p(u,t)\right\} \\ &+ \sum_k \nu_k(t)\,\left[p(u-w_k,t) - p(u,t)\right] \\ &+ A(t)\,\delta(u-u_r) - A(t)\,\delta(u-\theta_{\rm reset})\,.\end{aligned} \tag{13.14}$$

The first two terms on the right-hand side describe the continuous drift, the third term the jumps caused by stochastic spike arrival, and the last two terms take care of the reset. Because of the firing condition, we have $p(u,t) = 0$ for $u > \theta_{\rm reset}$.

Equations (13.13) and (13.14) can be used to predict the population activity $A(t)$ in a population of integrate-and-fire neurons stimulated by an arbitrary common input $I^{\rm ext}(t)$.

https://doi.org/10.1017/CBO9781107447615.016 Published online by Cambridge University Press

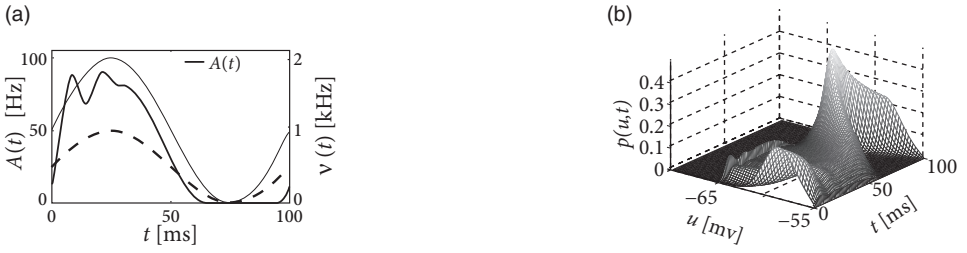

Fig. 13.3 Solution of the membrane potential density equation for time dependent input. The input is sinusoidal with a period of 100 ms. (a) Population activity $A(t)$ (thick solid line; left vertical scale) in response to excitatory and inhibitory spikes arriving with modulated firing rates (thin solid and dashed lines, respectively; right vertical scale). (b) The membrane population density $p(u,t)$ as a function of voltage and time during one period of the periodic stimulation. Adapted from Nykamp and Tranchina (2000) with kind permission from Springer Science and Business Media.

For a numerical implementation of Eq. (13.6) we refer the reader to the literature (Nykamp and Tranchina, 2000; Omurtag *et al*., 2000).

Example: Transient response of population activity

The population of 10 000 uncoupled leaky integrate-and-fire neurons simulated by Nykamp and Tranchina (2000) receives stochastic spike arrivals at excitatory and inhibitory synapses at rate $\nu_{\mathrm{E}}(t)$ and $\nu_{\mathrm{I}}(t)$, respectively. Each input spike causes a voltage jump of amplitude w. The raw jump size is drawn from some distribution and then multiplied with the difference between the synaptic reversal potential and value of the membrane potential just before spike arrival, so as to approximate the effect of conductance based synapses. The average jump size in the simulation was about 0.5 mV at excitatory synapses and -0.33 mV at inhibitory synapses (Nykamp and Tranchina, 2000).

The input rates are periodically modulated with frequency $f = 10$ Hz

$$\nu_{E/I}(t) = \bar{\nu}_{E/I}[1 + \sin(2\pi f t)], \tag{13.15}$$

with $\bar{\nu}_E = 2$ kHz and $\bar{\nu}_I = 1$ kHz. Integration of the population equations (13.13) and (13.14) yields a population activity $A(t)$ that responds strongly during the rising phase of the input, well before the excitatory input reaches its maximum; see Fig. 13.3a.

We compare the solution of the population activity equations with the explicit simulation of 10 000 uncoupled neurons. The simulated population activity of the finite network (Fig. 13.4a) is well approximated by the predicted activity $A(t)$ which becomes correct if the number of neurons goes to infinity. The density equations also predict the voltage distribution at each moment in time (Fig. 13.3b). The empirical histogram of voltages in a finite population of 10 000 neurons (Fig. 13.4b) is close to the smooth voltage distribution predicted by the theory.

https://doi.org/10.1017/CBO9781107447615.016 Published online by Cambridge University Press

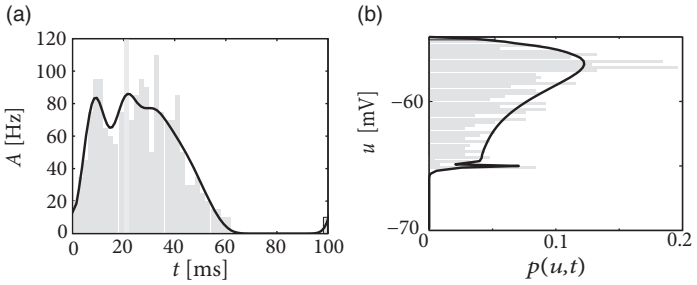

Fig. 13.4 Comparison of theory and simulation. (a) Population firing rate $A(t)$ as a function of time in a simulation of 100 neurons (gray histogram bars) compared to the prediction by the theory (solid line) while the population receives periodically modulated excitatory and inhibitory conductance input with period $T = 100$ ms. (b) Histogram of voltage distribution (gray horizontal bars) at $t_0 = 20$ ms in a population of 1000 neurons compared to the solution $p(u,t_0)$ of the density equation during the periodic stimulation. Adapted from Nykamp and Tranchina (2000) with kind permission from Springer Science and Business Media.

13.2.4 Single neuron versus population of neurons

Equation (13.14), which describes the dynamics of $p(u,t)$ in a population of integrate-and-fire neurons, is nearly identical to that of a single integrate-and-fire neuron with stochastic spike arrival; see Eq. (8.40). Apart from the fact that we have formulated the problem here for arbitrary nonlinear integrate-and-fire models, there are three subtle differences.

First, while $p(u,t)$ was introduced in Chapter 8 as *probability* density for the membrane potential of a *single* neuron, it is now interpreted as the density of membrane potentials in a large population of uncoupled neurons.

Second, the normalization is different. In Chapter 8, we considered a single neuron which was initialized at time $\hat{t}$ at a voltage u_r. For $t > \hat{t}$, the integrated density $\int_{-\infty}^{\theta_{\rm reset}} p(u,t)\, {\rm d}u \leq 1$ was interpreted as the probability that the neuron under consideration has not yet fired since its last spike at $\hat{t}$. The value of the integral therefore decreases over time. In the present treatment of a population of neurons, a neuron remains part of the population even if it fires. Thus the integral over the density remains constant over time; see Eq. (13.3).

Third, the fraction of neurons that "flow" across threshold per unit of time is the (expected value of) the population activity $A(t)$. Thus, the population activity has a natural interpretation in terms of the flux $J(\theta_{\rm reset},t)$.

13.3 Fokker–Planck equation

The equation for the membrane potential density in a population of integrate-and-fire neurons (see Eq. (13.14) in the previous section) can, in the limit of small jump amplitudes w_k, be approximated by a diffusion equation. To show this, we expand the right-hand side of Eq. (13.14) into a Taylor series up to second order in w_k. The result is the Fokker–Planck

https://doi.org/10.1017/CBO9781107447615.016 Published online by Cambridge University Press

equation,

$$\begin{aligned}\tau_m \frac{\partial}{\partial t} p(u,t) = &-\frac{\partial}{\partial u}\left\{\left[f(u) + RI^{\text{ext}}(t) + \tau_m \sum_k \nu_k(t)\, w_k\right] p(u,t)\right\} \\ &+ \frac{1}{2}\left[\tau_m \sum_k \nu_k(t)\, w_k^2\right] \frac{\partial^2}{\partial u^2} p(u,t) \\ &+ \tau_m A(t)\, \delta(u - u_r) - \tau_m A(t)\, \delta(u - \theta_{\text{reset}}) + \mathcal{O}(w_k^3)\,.\end{aligned} \tag{13.16}$$

The term with the second derivative describes a "diffusion" in terms of the membrane potential.

It is convenient to define the total "drive" in voltage units as

$$\mu(t) = RI^{\text{ext}}(t) + \tau_m \sum_k \nu_k(t)\, w_k \tag{13.17}$$

and the amount of diffusive noise (again in voltage units) as

$$\sigma^2(t) = \tau_m \sum_k \nu_k(t)\, w_k^2\,. \tag{13.18}$$

The firing threshold acts as an absorbing boundary so that the density at threshold vanishes:

$$p(\theta_{\text{reset}}, t) = 0\,. \tag{13.19}$$

The boundary condition $p(\theta_{\text{reset}}, t) = 0$ arises from the mathematical limiting process: We consider that all weights go to zero, $w_k \to 0$, while the total drive μ and the amount of diffusive noise remains constant. This is only possible if we have at least two different types of synapse (excitatory and inhibitory) and we increase the rate of both while decreasing the weights of synapses. In other words, the spike arrival rates at the synapses go to infinity so that the "shot noise" generated by spike arrivals turns into a white Gaussian distributed noise. Any neuron with a membrane potential just below the threshold would then immediately fire because of the noise. Therefore the density at the threshold has to be zero. This argument is no longer valid if spike arrival rates are finite, or if synapses react slowly so that the noise is colored (see Section 13.6.4 below).

In order to calculate the flux through the reset threshold we expand Eq. (13.13) in w_k about $u = \theta_{\text{reset}}$ and obtain

$$A(t) = -\left.\frac{\sigma^2(t)}{2\tau_m} \frac{\partial p(u,t)}{\partial u}\right|_{u=\theta_{\text{reset}}}, \tag{13.20}$$

Eqs. (13.16)–(13.20), together with the normalization (13.3), define the dynamics of a homogeneous population of integrate-and-fire neurons with "diffusive" noise. For a more detailed discussion of the diffusion limit see Chapter 8, in particular Eqs. (8.41) and (8.43).

https://doi.org/10.1017/CBO9781107447615.016 Published online by Cambridge University Press

Example: Flux in the diffusion limit

If we compare the continuity equation (13.7) with the explicit form of the Fokker–Planck equation (13.16), we can identify the flux caused by stochastic spike arrival and external current in the diffusion limit

$$J^{\rm diff}(u,t) = \frac{f(u)+\mu(t)}{\tau_m}\, p(u,t) - \frac{1}{2}\,\frac{\sigma^2(t)}{\tau_m}\,\frac{\partial}{\partial u} p(u,t). \qquad (13.21)$$

We emphasize that stochastic spike arrival contributes to the mean drive $\mu(t) = RI^{\rm ext}(t) + \tau_m \sum_k \nu_k(t)\, w_k$ as well as to the diffusive noise $\sigma^2(t) = \tau_m \sum_k \nu_k(t)\, w_k^2$.

13.3.1 Stationary solution for leaky integrate-and-fire neurons (*)

The stationary distribution $p(u)$ of the membrane potential is of particular interest, since it is experimentally accessible (Calvin and Stevens, 1968; Destexhe *et al.*, 2003; Crochet and Petersen, 2006). We now derive the stationary solution $p(u,t) \equiv p(u)$ of the Fokker–Planck equation (13.16) for a population of leaky integrate-and-fire neurons. Neurons are described by Eq. (13.1) with $f(u) = -u$, i.e., the voltage scale is shifted so that the equilibrium potential is at zero. For leaky integrate-and-fire neurons, the reset threshold is the same as the rheobase firing threshold and will be denoted by $\vartheta = \theta_{\rm reset} = \vartheta_{\rm rh}$.

We assume that the total input $h_0 = RI^{\rm ext} + \tau_m \sum_k \nu_k w_k$ is constant. In the stationary state, the temporal derivative on the left-hand side of Eq. (13.16) vanishes. The terms on the right-hand side can be transformed so that the stationary Fokker–Planck equation reads (for $u < \vartheta$)

$$0 = -\frac{\partial}{\partial u} J(u) + A_0\, \delta(u - u_r)\,, \qquad (13.22)$$

where A_0 is the population activity (or mean firing rate) in the stationary state and

$$J(u) = \frac{-u+h_0}{\tau_m}\, p(u) - \frac{1}{2}\,\frac{\sigma^2}{\tau_m}\,\frac{\partial}{\partial u} p(u) \qquad (13.23)$$

is the total flux; see Eqs. (13.6) and (13.21). The meaning of Eq. (13.22) is that the flux is constant except at $u = u_r$ where it jumps by an amount A_0. Similarly, the boundary condition $p(\vartheta,t) = 0$ implies a second discontinuity of the flux at $u = \vartheta$.

With the results from Chapter 8 in mind, we expect that the stationary solution approaches a Gaussian distribution for $u \to -\infty$. In fact, we can check easily that for any constant c_1

$$p(u) = \frac{c_1}{\sigma} \exp\left[-\frac{(u-h_0)^2}{\sigma^2}\right] \quad \text{for } u \le u_r \qquad (13.24)$$

is a solution of Eq. (13.22) with flux $J(u) = 0$. However, for $u > u_r$ a simple Gaussian distribution cannot be a solution since it does not respect the boundary condition $p(\vartheta) = 0$.

https://doi.org/10.1017/CBO9781107447615.016 Published online by Cambridge University Press

Nevertheless, we can make an educated guess and try a modified Gaussian (Giorno *et al.*, 1992; Brunel and Hakim, 1999)

$$p(u) = \frac{c_2}{\sigma^2} \exp\left[-\frac{(u-h_0)^2}{\sigma^2}\right] \cdot \int_u^\vartheta \exp\left[\frac{(x-h_0)^2}{\sigma^2}\right] \mathrm{d}x \quad \text{for } u_r < u \le \vartheta\,, \tag{13.25}$$

with some constant c_2. We have written the above expression as a product of two terms. The first factor on the right-hand side is a standard Gaussian while the second factor guarantees that $p(u) \to 0$ for $u \to \vartheta$. If we insert Eq. (13.25) in (13.22) we can check that it is indeed a solution. The constant c_2 is proportional to the flux,

$$c_2 = 2\,\tau_m J(u) \quad \text{for } u_r < u \le \vartheta\,. \tag{13.26}$$

The solution defined by Eqs. (13.24) and (13.25) must be continuous at $u = u_r$. Hence

$$c_1 = \frac{c_2}{\sigma} \int_{u_r}^\vartheta \exp\left[\frac{(x-h_0)^2}{\sigma^2}\right] \mathrm{d}x\,. \tag{13.27}$$

Finally, the constant c_2 is determined by the normalization condition (13.3). We use Eqs. (13.24), (13.25), and (13.27) in (13.3) and find

$$\frac{1}{c_2} = \int_{-\infty}^{u_r}\int_{u_r}^\vartheta f(x,u)\,\mathrm{d}x\mathrm{d}u + \int_{u_r}^\vartheta\int_u^\vartheta f(x,u)\,\mathrm{d}x\mathrm{d}u = \int_{u_r}^\vartheta\int_{-\infty}^x f(x,u)\,\mathrm{d}u\mathrm{d}x\,, \tag{13.28}$$

with

$$f(x,u) = \frac{1}{\sigma^2} \exp\left[-\frac{(u-h_0)^2}{\sigma^2}\right] \exp\left[\frac{(x-h_0)^2}{\sigma^2}\right]. \tag{13.29}$$

Figure 13.5b shows the resulting stationary density $p(u)$ for different noise amplitudes.

The activity A_0 is identical to the flux $J(u)$ between u_r and ϑ and therefore proportional to the constant c_2; see Eq. (13.26). If we express the integral over u in Eq. (13.28) in terms of the error function, $\mathrm{erf}(x) = \frac{2}{\sqrt{\pi}} \int_0^x \exp(-u^2)\,\mathrm{d}u$, we obtain

$$A_0^{-1} = \tau_m \sqrt{\pi} \int_{\frac{u_r-h_0}{\sigma}}^{\frac{\vartheta-h_0}{\sigma}} \exp\left(x^2\right) \left[1 + \mathrm{erf}(x)\right] \mathrm{d}x\,, \tag{13.30}$$

which is identical to the Siegert formula (Siegert, 1951) of the single-neuron firing rate [see Eq. (8.54) or (12.26)] that we used previously in Chapters 8 and 12. An alternative formulation (see Exercises) of the remaining integral in Eq. (13.30) is also possible (Brunel and Hakim, 1999).

13.4 Networks of leaky integrate-and-fire neurons

In the previous section, the formalism of membrane potential densities was applied to a single population driven by spikes arriving at some rate ν_k at the synapse of type k, where $k = 1, \ldots, K$. In a population that is coupled to itself, the spikes that drive a given neuron

https://doi.org/10.1017/CBO9781107447615.016 Published online by Cambridge University Press

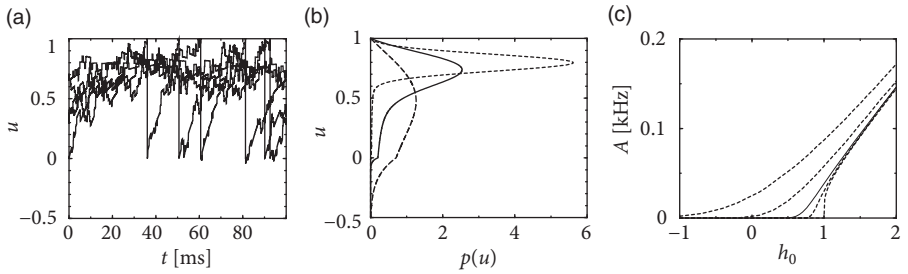

Fig. 13.5 (a) Membrane potential trajectories of five neurons ($R = 1$ and $\tau_m = 10\,\text{ms}$) driven by a constant background current $I_0 = 0.8$ and stochastic background input with $\nu_+ = \nu_- = 0.8\,\text{kHz}$ and $w_\pm = \pm 0.05$. These parameters correspond to $h_0 = 0.8$ and $\sigma = 0.2$ in the diffusive noise model. (b) Stationary membrane potential distribution in the diffusion limit for $\sigma = 0.2$ (solid line), $\sigma = 0.1$ (short-dashed line), and $\sigma = 0.5$ (long-dashed line). (Threshold $\vartheta = 1$.) (c) Mean activity of a population of integrate-and-fire neurons with diffusive noise as a function of h_0 for four different noise levels: (from top to bottom) $\sigma = 1.0, \sigma = 0.5, \sigma = 0.2$ (solid line), $\sigma = 0.1, \sigma = 0.0$.

are, at least partially, generated within the same population. For a homogeneous population with self-coupling the feedback is then proportional to the population activity $A(t)$; see Chapter 12.

We now formulate the interaction between several coupled populations using the Fokker–Planck equation for the membrane potential density (Section 13.4.1) and apply it subsequently to the special cases of a population of excitatory integrate-and-fire neurons interacting with a population of inhibitory ones (Section 13.4.2).

13.4.1 Multiple populations

We consider multiple populations $k = 1, \ldots, K$. The population with index k contains N_k neurons and its activity is denoted by A_k. We recall that $N_k A_k(t)\,\Delta t$ is the total number of spikes emitted by population k in a short interval Δt.

Let us suppose that population k sends its spikes to another population n. If each neuron in population n receives input from *all* neurons in k the total spike arrival rate from population k is therefore $\nu_k(t) = N_k A_k(t)$ ("full connectivity"). If each neuron in population n receives connections only from a subset of C_{nk} randomly chosen neurons of population k, then the total spike arrival rate is $\nu_k(t) = C_{nk} A_k(t)$ ("random connectivity" with a connection probability $p_{nk} = C_{nk}/N_k$ from population k to population n). We assume that all connections from k to n have the same weight w_{nk} and that spike arrival from population k can be approximated by a Poisson process with rate $\nu_k(t)$.

For each population $n = 1, \ldots, K$ we write down a Fokker–Planck equation analogous to Eq. (13.16). Neurons are leaky integrate-and-fire neurons. Within a population n, all neurons have the same parameters τ_n, R_n, u_r^n, and in particular the same firing threshold ϑ_n. For population n the Fokker–Planck equation for the evolution of membrane potential

https://doi.org/10.1017/CBO9781107447615.016 Published online by Cambridge University Press

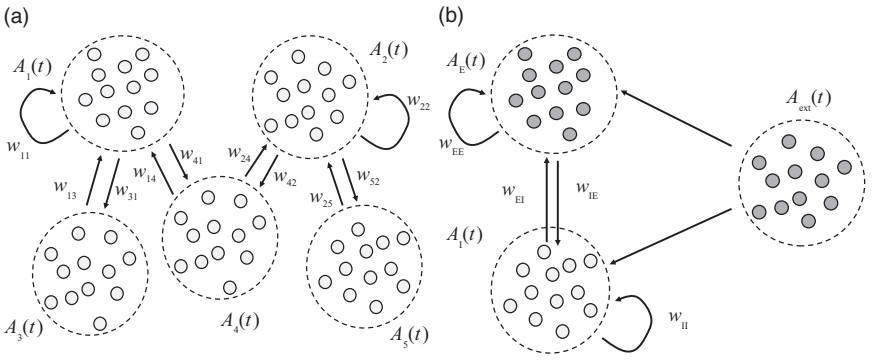

Fig. 13.6 Interacting populations. (a) Five populations interact via their population activities A_k. The parameter w_{nk} gives the synaptic weight of a connection from a presynaptic neuron in population k to a postsynaptic neuron in population n. Not all populations are coupled with each other. (b) Brunel network: an excitatory population of leaky integrate-and-fire neurons is coupled to itself and to an inhibitory population. Neurons in both populations receive also external input from a third population with population activity $A_{\text{ext}} = \nu^{\text{ext}}$ described as a homogeneous Poisson process.

densities is then

$$\begin{aligned}\tau_n \frac{\partial}{\partial t} p_n(u,t) = -\frac{\partial}{\partial u}\left\{\left[-u + R_n I_n^{\text{ext}}(t) + \tau_n \sum_k C_{nk} A_k(t)\, w_{nk}\right] p_n(u,t)\right\} \\ + \frac{1}{2}\left[\tau_n \sum_k C_{nk} A_k(t)\, w_{nk}^2\right] \frac{\partial^2}{\partial u^2} p_n(u,t) \\ + \tau_n A_n(t)\, \delta(u - u_r^n) - \tau_n A_n(t)\, \delta(u - \vartheta_n)\,.\end{aligned} \tag{13.31}$$

The population activity A_n is the flux through the threshold (see Eq. (13.20)), which gives in our case

$$A_n(t) = -\frac{1}{2}\left[\sum_k C_{nk} A_k(t)\, w_{nk}^2\right] \left(\frac{\partial p_n(u,t)}{\partial u}\right)_{u=\vartheta_n}. \tag{13.32}$$

Thus populations interact with each other via the variable $A_k(t)$; see Fig. 13.6.

Example: Background input

Sometimes it is useful to focus on a single population, coupled to itself, and replace the input arising from other populations by background input. For example, we may focus on population $n = 1$, which is modeled by Eq. (13.31), but use as the inputs A_k spikes generated by a homogeneous or inhomogeneous Poisson process with rate $A_k = \nu_k$.

https://doi.org/10.1017/CBO9781107447615.016 Published online by Cambridge University Press

Example: Full coupling and random coupling

Full coupling can be retrieved by setting $C_{nk} = N_k$ and $w_{nk} = J_{nk}/N_k$. In this case the amount of diffusive noise in population n,

$$\sigma_n^2(t) = \tau_n \left[\sum_k C_{nk} A_k(t) \, w_{nk}^2 \right] , \tag{13.33}$$

decreases with increasing population size $\sigma_n^2 \propto 1/N_k$.

13.4.2 Synchrony, oscillations, and irregularity

In Chapter 12 we have already discussed the stationary state of the population activity in a population coupled to itself. With the methods discussed in Chapter 12 we were, however, unable to study the stability of the stationary state; nor were we able to make any prediction about potential time-dependent solutions.

We now give a more complete characterization of a network of leaky integrate-and-fire neurons consisting of two populations: a population of N_E excitatory neurons coupled to a population with $N_\mathrm{I} = N_\mathrm{E}/4$ inhibitory neurons (Brunel, 2000). The structure of the network is shown in Fig. 13.6b. Each neuron (be it excitatory or inhibitory) receives C_E connections from the excitatory population, each with weight $w_{EE} = w_{IE} = w_0$; it also receives $C_I = C_E/4$ connections from the inhibitory population ($w_{EI} = w_{II} = -g\,w_0$) and furthermore C_E connections from an external population (weight w_{EE}) with neurons that fire at a fixed rate ν^ext. Each spike causes, after a delay of $\Delta = 1.5\,\mathrm{ms}$ a voltage jump of $w_0 = 0.1\,\mathrm{mV}$ and the threshold is $20\,\mathrm{mV}$ above resting potential. Note that each neuron receives four times as many excitatory than inhibitory inputs so that the total amount of inhibition balances excitation if inhibition is four times stronger ($g = 4$), but the relative strength g is kept as a free parameter. Also note that, in contrast to Chapter 12, the weight here has units of voltage and directly gives the amplitude of the voltage jump: $w_0 = \Delta u_E$.

The population can be in a state of asynchronous irregular activity (AI), where neurons in the population fire at different times ("asynchronous" firing) and the distribution of interspike intervals is fairly broad ("irregular" firing of individual neurons); see Fig. 13.7b. This is the state that corresponds to the considerations of stationary activity in Chapter 12. However, with a slight change of parameters, the same network can also be in a state of fast synchronous regular (SR) oscillations. It is characterized by periodic oscillations of the population activity *and* a sharply peaked interval distribution of individual neurons. The network can also be in the state of synchronous irregular firing (SI) either with fast (SI fast) or with slow (SI slow) oscillations of the population activity. The oscillatory temporal structure emerges despite the fact that the input has a constant spike arrival rate. It can be traced back to an instability of the asynchronous firing regime toward oscillatory activity.

With the mathematical approach of the Fokker–Planck equations, it is possible to determine the instabilities analytically. The mathematical approach will be presented in

https://doi.org/10.1017/CBO9781107447615.016 Published online by Cambridge University Press

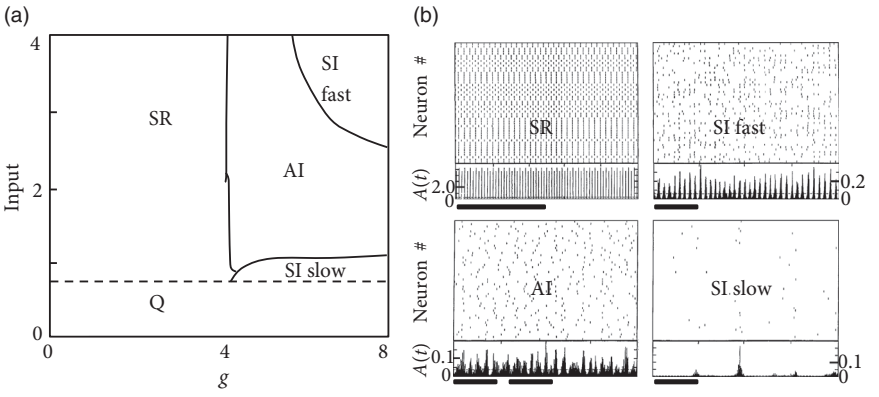

Fig. 13.7 Population of pulse-coupled leaky integrate-and-fire neurons (Brunel network). (a) Phase diagram of the Brunel network. The population activity can be in a state of asynchronous irregular (AI), synchronous regular (SR) or synchronous irregular (SI) activity. The horizontal axis indicates the relative importance of inhibition ($g = 4$ corresponds to balance between excitation and inhibition). The vertical axis is the amount of external input each neuron receives. Input $I = 1$ corresponds to a mean input just sufficient to reach the neuronal firing threshold (in the absence of recurrent input from the network). Stability of the asynchronous irregular firing state (AI) breaks down at the dashed or solid lines and can lead to synchronous regular (SR), or synchronous irregular (SI, either fast or slow) activity, or to a near-quiescent state (Q); redrawn after Brunel (2000). (b) Typical time course of the population activity $A(t)$ (bottom part of each subgraph, units in kHz) and associated spike patterns (50 randomly chosen neurons are plotted along the vertical axis in the top part of each subgraph; each dot indicates a spike) in different firing regimes. "SI fast" refers to fast and regular oscillations, but individual neurons fire irregularly with intervals at random multiples of the oscillation period. Horizontal black bar: 50 ms. Simulation of 10 000 excitatory and 2500 inhibitory neurons with connection probability $p = 0.1$. Each spike causes, after a delay of $\Delta = 1.5$ ms a voltage jump of 0.1 mV; distance from equilibrium potential to the threshold is 20 mV; absolute refractory period 2 ms; membrane time constant 20 ms. Parameters are top left: $g = 3$, input = 2 (SR); top right: $g = 6$, input = 4 (SI fast); bottom left: $g = 5$, input = 2 (AI) bottom right $g = 4.5$, input = 0.9 (SI slow). Adapted from Brunel (2000) with kind permission from Springer Science and Business Media.

Section 13.5.2, but Fig. 13.7a already shows the result. Stability of a stationary state of asynchronous firing is most easily achieved in the regime where inhibition dominates excitation. Since each neuron receives four times as many excitatory as inhibitory inputs, inhibition must be at least four times as strong ($g > 4$) as excitation. In order to get nonzero activity despite the strong inhibition, the external input alone must be sufficient to make the neurons fire. "Input = 1" corresponds to an average external input just sufficient to reach the firing threshold, without additional input from the network.

Consider now the regime of strong inhibition ($g > 4$) and strong input, say spikes from the external source arrive at a rate leading to a mean input of amplitude 4. To understand how the network can run into an instability, let us consider the following intuitive argument. Suppose a momentary fluctuation leads to an increase in the total amount of activity in the

https://doi.org/10.1017/CBO9781107447615.016 Published online by Cambridge University Press

excitatory population. This causes, after a transmission delay Δ, an increase in inhibition and, after a further delay Δ, a suppression of excitation. If this feedback loop is strong enough, an oscillation with period 4Δ may appear, leading to fast-frequency ("SI fast") oscillations (Brunel, 2000).

If the external input is, on its own, not sufficient to keep the network going ("input < 1"), then a similar small fluctuation may eventually turn the network from a self-activated state into a quiescent state where the only activity is that caused by external input. It then needs another fluctuation (caused by variations of spike arrivals from the external source) to kick it back into a short burst of activity (Brunel, 2000). This leads to slow irregular but synchronous bursts of firing ("SI slow").

Finally, if inhibition is globally weak compared to excitation ($g < 4$), then the population is in a state of high activity where each neuron fires close to its maximal rate (set by the inverse of an absolute refractory period). This high-activity state is unstable compared to fast but regular oscillations ("SR"). Typically, the population can split up into two or more subgroups, the number of which depends on the transmission delay (Brunel, 2000; Gerstner and van Hemmen, 1993).

Example: Analysis of the Brunel network

All neurons have the same parameters, so that we can assume that they all fire at the same time-dependent firing rate $\nu(t) = A(t)$. We assume that the network is large $N \gg C_{\mathrm{E}}$, so that it is unlikely that neurons share a large fraction of presynaptic neurons; therefore inputs can be considered as uncorrelated, except for the trivial correlations induced by their common modulation of the firing rate $A(t)$.

The mean input at time t to a neuron in either the excitatory or the inhibitory population is (in voltage units)

$$\mu(t) = \tau_m w_0 C_E [1 - g/4] A(t-\Delta) + \tau_m w_0 C_E \nu^{\mathrm{ext}}, \tag{13.34}$$

and the input also generates diffusive noise (in voltage units) of strength

$$\sigma^2(t) = \tau_m w_0^2 C_E [(1 + g^2/4) A(t-\Delta) + \nu_{\mathrm{ext}}]. \tag{13.35}$$

The mean and σ^2 are inserted in the Fokker–Planck equation (see Eq. 13.31)

$$\begin{aligned} \tau_m \frac{\partial}{\partial t} p(u,t) = &- \frac{\partial}{\partial u} \{[-u + \mu(t)]\, p(u,t)\} \\ &+ \frac{1}{2} \sigma^2(t) \frac{\partial^2}{\partial u^2} p(u,t) \\ &+ \tau_m A(t)\, \delta(u - u_r) - \tau_m A(t)\, \delta(u - \vartheta) + \mathcal{O}(w_k^3). \end{aligned} \tag{13.36}$$

The main difference to the stationary solution considered in Section 13.3.1 and Chapter 12 is that mean input and noise amplitude are kept time-dependent.

We first solve to find the stationary solution of the Fokker–Planck equation, denoted as $p_0(u)$ and activity A_0. This step is completely analogous to the calculation in Section 13.3.1.

https://doi.org/10.1017/CBO9781107447615.016 Published online by Cambridge University Press

In order to analyze the stability of the stationary solution, we search for solutions of the form $A(t) = A_0 + A_1 e^{\lambda t} \cos(\omega t)$ (for details, see Section 13.5.2). Parameter combinations that lead to a value $\lambda > 0$ indicate an instability of the stationary state of asynchronous firing for a network with this set of parameters.

Figure 13.7a indicates that there is a broad regime of *stability* of the asynchronous irregular firing state (AI). This holds even if the network is completely deterministic (Brunel, 2000) and driven by a constant input I_0 (i.e., we set $\nu^{\text{ext}} = 0$ in the noise term, Eq. (13.35), and replace spike arrivals by a constant current $RI_0^{\text{ext}} = w_0 C_{\text{E}} \nu^{\text{ext}}$ in Eq. (13.34).

Stability of the stationary state of asynchronous irregular activity is most easily achieved if the network is in the regime where inhibition slightly dominates excitation and external input is sufficient to drive neurons to the threshold. This is called the "inhibition dominating" regime. The range of parameters where asynchronous firing is stable can, however, be increased into the range of dominant excitation, if delays are not fixed at $D = 1.5$ ms, but drawn from the range $0 < D < 3$ ms. Finite size effects can also be taken into account (Brunel, 2000).

13.5 Networks of nonlinear integrate-and-fire neurons

In Chapter 5 it was shown that nonlinear integrate-and-fire neurons such as the exponential integrate-and-fire model provide an excellent approximation to the dynamics of single neurons, much better than the standard leaky integrate-and-fire model. This section indicates how the Fokker–Planck approach can be used to analyze networks of such nonlinear integrate-and-fire models.

We determine, for arbitrary nonlinear integrate-and-fire models driven by a diffusive input with constant mean $\mu = RI_0$ and noise σ^2, the distribution of membrane potentials $p_0(u)$ as well as the linear response of the population activity

$$A(t) = A_0 + A_1(t) = A_0 + \int_0^\infty G(s)\, I_1(t-s)\, \mathrm{d}s \tag{13.37}$$

to a drive $\mu(t) = R[I_0 + I_1(t)]$ (Richardson, 2007). As explained in Section 13.4, knowledge of p_0 is sufficient to predict, for coupled populations of integrate-and-fire neurons, the activity A_0 in the stationary state of asynchronous firing. Moreover, we shall see that the filter $G(s)$ contains all the information needed to analyze the stability of the stationary state of asynchronous firing. In this section we focus on one-dimensional nonlinear integrate-and-fire models, and add adaptation later on, in Section 13.6.

13.5.1 Steady-state population activity

We consider a population of nonlinear integrate-and-fire models in the diffusion limit. We start with the continuity equation (13.7)

https://doi.org/10.1017/CBO9781107447615.016 Published online by Cambridge University Press

$$\frac{\partial}{\partial t}p(u,t) = -\frac{\partial}{\partial u}J(u,t) + A(t)\,\delta(u-u_r) - A(t)\,\delta(u-\theta_{\text{reset}})\,. \tag{13.38}$$

In the stationary state, the membrane potential density does not depend on time, $p(u,t) = p_0(u)$, so that the left-hand side of (13.38) vanishes. Eq. (13.38) therefore simplifies to

$$\frac{\partial}{\partial u}J(u,t) = A(t)\,\delta(u-u_r) - A(t)\,\delta(u-\theta_{\text{reset}})\,. \tag{13.39}$$

Therefore the flux takes a constant value, except at two values: at the numerical threshold θ_{reset}, at which the membrane potential is reset; and at the potential u_r, to which the reset occurs. The flux vanishes for $u > \theta_{\text{reset}}$ and for $u < u_r$. For $u_r < u < \theta_{\text{reset}}$ the constant value $J(u,t) = c > 0$ still needs to be determined.

A neuron in the population under consideration is driven by the action potentials emitted by presynaptic neurons from the same or other populations. For stochastic spike arrivals at rate ν_k, where each spike causes a jump of the voltage by an amount w_k, the contributions to the flux have been determined in Eqs. (13.10) and (13.11). In the diffusion limit the flux according to Eq. (13.21) is

$$J(u,t) = \frac{1}{\tau_m}\left[f(u) + \mu(t) - \frac{1}{2}\sigma^2(t)\frac{\partial}{\partial u}\right]p(u,t)\,. \tag{13.40}$$

In the stationary state, we have $p(u,t) = p_0(u)$ and $J(u,t) = c$ for $u_r < u < \theta_{\text{reset}}$. (For $u < u_r$ we have $J(u,t) = 0$.) Hence Eq. (13.40) simplifies to a first-order differential equation

$$\frac{\mathrm{d}p_0(u)}{\mathrm{d}u} = \frac{2\tau_m}{\sigma^2}\left[\frac{f(u)+\mu}{\tau_m}p_0(u) - c\right]. \tag{13.41}$$

The differential equation (13.41) can be integrated numerically starting at the upper bound $u = \theta_{\text{reset}}$ with initial condition $p_0(\theta_{\text{reset}}) = 0$ and $\mathrm{d}p_0/\mathrm{d}u|_{\theta_{\text{reset}}} = -1 = -2c\tau_m/\sigma^2$. When the integration passes $u = u_r$ the constant switches from c to zero. The integration is stopped at a lower bound u_{low} when p_0 has approached zero. The exact value of the lower bound is of little importance.

At the end of the integration, the surface under the voltage distribution $\int_{u_{\text{low}}}^{\theta_{\text{reset}}} p_0(u)\mathrm{d}u = 1$, which determines the constant c and therefore the firing rate A_0 in the stationary state.

Example: Exponential integrate-and-fire model

The exponential integrate-and-fire model (Fourcaud-Trocme *et al.*, 2003) as defined in Eq. (5.6) is characterized by the differential equation

$$\tau\frac{\mathrm{d}}{\mathrm{d}t}u = -(u-u_{\text{rest}}) + \Delta_T\exp\left(\frac{u-\vartheta_{\text{rh}}}{\Delta_T}\right) + \mu\,, \tag{13.42}$$

where μ is the total drive in units of the membrane potential. The result of the numerical integration of Eqs. (13.39) and (13.41) depends critically on the relative value of the reset potential, the driving potential μ with respect to the reset u_r, and the rheobase firing

https://doi.org/10.1017/CBO9781107447615.016 Published online by Cambridge University Press

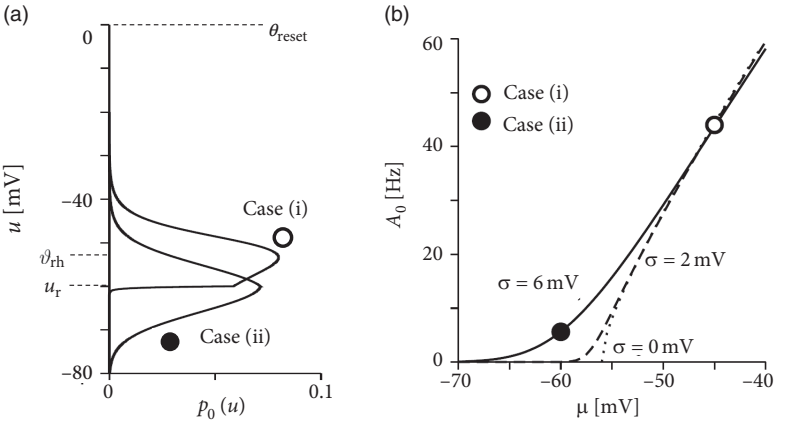

Fig. 13.8 Exponential integrate-and-fire neurons. (a) The stationary membrane potential density $p_0(u)$ in the regime of low noise and superthreshold drive (case (i): $\sigma = 2$ mV, $\mu = -45$ mV $> \vartheta_{rh} = -53$ mV $> u_r = -60$ mV) and in the regime of high noise and subthreshold drive (case (ii): $\sigma = 6$ mV, $\mu = u_r = -60$ mV $< \vartheta_{rh} = -53$ mV). Note that the exact value of the numerical firing threshold ($\theta_{reset} = 0$ mV) is irrelevant because the membrane $p_0(u)$ is, for all potentials above -30 mV, very small. (b) The stationary population firing rate $A_0 = g_\sigma(I_0)$ as a function of the total drive $\mu = RI_0$ of the population, in the regimes of high noise (solid line, $\sigma = 6$ mV), low noise (dashed line, $\sigma = 2$ mV), and in the absence of noise (dotted, $\sigma = 0$). The two cases depicted in (a) are marked by open and solid symbols. Adapted from Richardson (2007).

threshold ϑ_{rh}, as well as on the level σ of diffusive noise. Two representative scenarios are shown in Fig. 13.8a. Case (i) has very little noise ($\sigma = 2$ mV) and the total drive ($\mu = -45$ mV) is above the rheobase firing threshold ($\vartheta_{rh} = -53$ mV). In this case, the membrane potential density a few millivolts below the reset potential ($u_r = -60$ mV) is negligible. Because of the strong drive, the model neuron model is in the superthreshold regime (see Section 8.3) and fires regularly with a rate of about 44 Hz.

Case (ii) is different, because it has a larger amount of noise ($\sigma = 6$ mV) and a negligible drive of $\mu = u_r = -60$ mV. Therefore, the distribution of membrane potentials is broad, with a maximum at u_r, and firing is noise driven and occurs at a low rate of 5.6 Hz.

For both noise levels, the frequency–current curve $A_0 = \nu = g_\sigma(I_0)$ is shown in Fig. 13.8b, as a function of the total drive $\mu = RI$. We emphasize that for very strong superthreshold drive, the population firing rate A_0 of noisy neurons is lower than that of noise-free neurons.

13.5.2 Response to modulated input (*)

So far we have restricted the discussion to a constant input I_0. We now add a small periodic perturbation

$$I(t) = I_0 + \varepsilon \cos(\omega t), \tag{13.43}$$

https://doi.org/10.1017/CBO9781107447615.016 Published online by Cambridge University Press

where $\omega = 2\pi/T$; the parameter T denotes the period of the modulation. We expect the periodic drive to lead to a small periodic change in the population activity

$$A(t) = A_0 + A_1(\omega)\cos(\omega t + \phi_A(\omega)). \tag{13.44}$$

Our aim is to calculate the complex number $\hat{G}$ that characterizes the linear response or "gain" at frequency ω

$$\hat{G}(\omega) = \frac{A_1(\omega)}{\varepsilon} e^{i\phi_A(\omega)}. \tag{13.45}$$

The result for a population of exponential integrate-and-fire neurons is shown in Fig. 13.9.

Once we have found the gain $\hat{G}$ for arbitrary frequencies ω, an inverse Fourier transform of $\hat{G}$ gives the linear filter $G(s)$. The linear response of the population activity $A(t) = A_0 + \Delta A(t)$ to an *arbitrary* input current $I(t) = I_0 + \Delta I(t)$ is

$$\Delta A(t) = \int_0^\infty G(s)\,\Delta I(t-s)\,\mathrm{d}s. \tag{13.46}$$

A linear response is a valid description if the change is small:

$$\Delta A(t) \ll A(t). \tag{13.47}$$

In our case of periodic stimulation, the amplitude of the input current is scaled by ε. We are free to choose ε small enough to fulfill condition (13.47).

The small periodic drive at frequency ω leads to a small periodic change in the density of membrane potentials

$$p(u,t) = p_0(u) + p_1(u)\cos(\omega t + \phi_p(u)), \tag{13.48}$$

which has a phase lead ($\phi_p > 0$) or lag ($\phi_p < 0$) with respect to the periodic drive. We assume that the modulation amplitude in the input current ε is small so that $p_1(u) \ll p_0(u)$ for most values of u. We say that the change is at most of "order ε."

Similarly to the membrane potential density, the flux $J(u,t)$ will also exhibit a small perturbation of order ε. For the exponential integrate-and-fire model of Eq. (13.42) with $u_{\rm rest} = 0$ the flux is (see Eq. (13.40))

$$J(u,t) = \left[\frac{-u + RI(t)}{\tau_m} + \frac{\Delta_T}{\tau_m}\exp\left(\frac{u-\vartheta_{\rm rh}}{\Delta_T}\right) - \frac{\sigma^2(t)}{2\tau_m}\frac{\partial}{\partial u}\right] p(u,t) = Q(u,t)\,p(u,t), \tag{13.49}$$

where we have introduced on the right-hand side a linear operator Q that comprises all the terms inside the square brackets. The stationary state that we analyzed in the previous subsection under the assumption of constant input $I(t) = I_0$ has a flux $J_0(u) = Q_0(u)\,p_0(u)$. In the presence of the periodic perturbation, the flux is

$$J(u,t) = J_0(u) + J_1(u)\cos(\omega t + \phi_J(u)) \tag{13.50}$$

with

$$J_1(u)\cos(\omega t + \phi_J(u)) = Q_0(u)\,p_1(u)\cos(\omega t + \phi_p(u)) + Q_1(u,t)\,p_0(u) + 0_{\rm order}(\varepsilon^2), \tag{13.51}$$

https://doi.org/10.1017/CBO9781107447615.016 Published online by Cambridge University Press

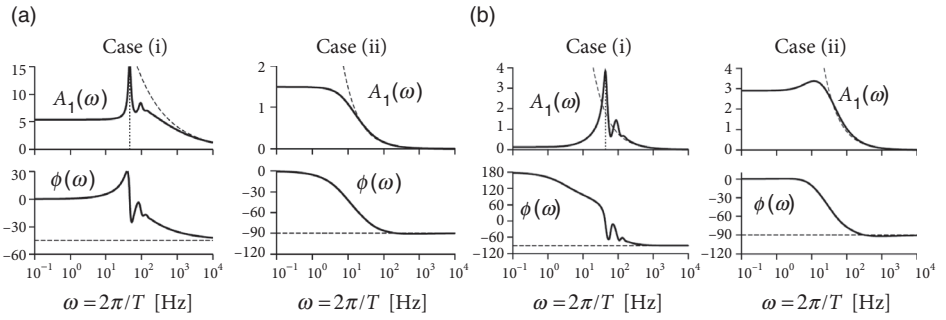

Fig. 13.9 Frequency response of a population of exponential integrate-and-fire neurons, with parameter settings as in Fig. 13.8. Solid line: theoretical Dashed line: analytical prediction for high frequencies. (a) Case (i): The population response $A_1(\omega)$ (top) to a periodic stimulation of frequency $\omega = 2\pi/T$ in the situation of low noise ($\sigma = 2$ mV) shows a resonance at the population firing rate $A_0 = 44$ Hz. The phase shift $\phi(\omega)$ for low noise (bottom) approaches -45° for high frequencies. Case (ii): The population response $A_1(\omega)$ for high noise ($\sigma = 6$ mV, population firing rate $A_0 = 5.6$ Hz) has no resonance (top) and the phase shift $\phi(\omega)$ approaches -90° (bottom). The combination of amplitude and phase $A_1(\omega)\exp(i\phi(\omega))$ defines the complex frequency-dependent gain factor $\hat{G}(\omega)$ in response to modulation of the input current. (b) Gain factor G_σ for a modulation of the noise strength $\sigma^2(t)$ while the input current is constant. Case (i): low noise. Case (ii): high noise. (a) and (b) adapted from Richardson (2007). © 2007 The American Physical Society.

where $Q_1(u,t) = \varepsilon R\cos(\omega t)/\tau_m$ is the change of the operator Q to order ε. Note that the flux through the threshold $\theta_{\rm reset}$ gives the periodic modulation of the population activity.

We insert our variables A, p, J into the differential equation (13.38) and find that the stationary terms with subscript zero cancel each other, as should be the case, and only the terms with subscript "1" survive. To simplify the notation, it is convenient to switch from real to complex numbers and include the phase in the definition of $A_1, p_1(u), J_1(u)$, for example, $\hat{A}_1 = A_1\exp(i\phi_A)$; the hat indicates the complex number. If we take the Fourier transform over time, Eq. (13.38) becomes

$$-\frac{\partial}{\partial u}\hat{J}_1(u) = i\omega\hat{p}_1(u) + \hat{A}_1\left[\delta(u-\theta_{\rm reset}) - \delta(u-u_r)\right]. \qquad (13.52)$$

Before we proceed further, let us have a closer look at Eqs. (13.51) and (13.52). We highlight three aspects (Richardson, 2007). The first observation is that we have, quite arbitrarily, normalized the membrane potential density to an integral of unity. We could have chosen, with equal rights, a normalization to the total number N of neurons in the population. Then the flux on the left-hand side of Eq. (13.52) would be enlarged by a factor of N, but so would the membrane potential density and the population activity, which appear on the right-hand side. We could also multiply both sides of the equation by any other (complex) number. As a consequence, we can, for example, try to solve Eq. (13.52) for a population activity modulation $\hat{A}_1 = 1$ and take care of the correct normalization only later.

The second observation is that the flux J_1 in Eq. (13.51) can be quite naturally separated into two components. The first contribution to the flux is proportional to the perturbation p_1 of the membrane potential density. The second component is caused by the direct action of the external current $Q_1(u,t) = \varepsilon R \cos(\omega t)/\tau_m$. We will exploit this separability of the flux later.

The third observation is that, for the case of exponential integrate-and-fire neurons, the explicit expression for the operators Q_0 and Q_1 can be inserted into Eq. (13.51), which yields a first-order differential equation

$$\frac{\partial}{\partial u}\hat{p}_1(u) = \frac{2}{\sigma^2}\left[-u + RI_0 + \Delta_T \exp\left(\frac{u-\vartheta_{\rm rh}}{\Delta_T}\right)\right]\hat{p}_1(u) + \frac{2R\varepsilon}{\sigma^2}\,p_0(u) - \frac{2\tau_m}{\sigma^2}\,\hat{J}_1(u). \tag{13.53}$$

We therefore have two first-order differential equations (13.52) and (13.53) which are coupled to each other. In order to solve the two equations, we now exploit our second observation and split the flux into two components. We drop the hats on J_1, p_1, A_1 to lighten the notation.

(i) A "free" component $J_1^{\rm free}(u)$ describes the flux that would occur in the absence of external drive ($\varepsilon = 0$), but in the presence of a periodically modulated population activity A_1. Intuitively, the distribution of the membrane potential density $p_1^{\rm free}(u)$ and the flux $J_1^{\rm free}$ must exhibit some periodic "breathing pattern" to enable the periodic modulation of the flux through the threshold of strength $\hat{A}_1$. We find the "free" component by integrating Eq. (13.53) with $\varepsilon = 0$ in parallel with Eq. (13.52) with parameter $A_1 = 1$ (i.e., the periodic flow through threshold is of unit strength). The integration starts at the initial condition $p_1(\theta_{\rm reset}) = 0$ and $J_1^{\rm free}(\theta_{\rm reset}) = A_1 = 1$ and continues toward decreasing voltage values. Integration stops at a lower bound $u_{\rm low}$ which we place at an arbitrarily large negative value.

(ii) A "driven" component J_1^{ε} accounts for the fact that the periodic modulation is in fact caused by the input. We impose for the "driven" component that the modulation of the flux through threshold vanishes: $A_1 = 0$. We can therefore find the "driven" component by integrating Eq. (13.53) with a finite $\varepsilon > 0$ in parallel with Eq. (13.52) with parameter $A_1 = 0$ starting at the initial condition $p_1(\theta_{\rm reset}) = 0$ and $J_1^{\varepsilon}(\theta_{\rm reset}) = A_1 = 0$ and integrating toward decreasing voltage values. As before, integration stops at a lower bound $u_{\rm low}$ which we can shift to arbitrarily large negative values.

Finally we add the two solutions together: any combination of parameters a_1, a_2 for the total flux $a_1 J_1^{\rm free}(u) + a_2 J_1^{\varepsilon}(u)$ and the total density $a_1 p_1^{\rm free}(u) + a_2 p_1^{\varepsilon}(u)$ will solve the pair of differential equations (13.53) and (13.52). Which one is the right combination?

The total flux must vanish at large negative values. Therefore we require a boundary condition

$$0 = J(u_{\rm low}) = a_1 J_1^{\rm free}(u_{\rm low}) + a_2 J_1^{\varepsilon}(u_{\rm low})\,. \tag{13.54}$$

We recall that $J_1^{\varepsilon}(u)$ is proportional to the drive ε. Furthermore, the initial condition was chosen such that $J_1^{\rm free}(\theta_{\rm reset})$ yields a population response $A_1 = 1$ so that, in the combined solution, the factor a_1 is the population response!

https://doi.org/10.1017/CBO9781107447615.016 Published online by Cambridge University Press

We are interested in the "gain factor" at stimulation frequency ω. We started this section by applying a periodic stimulus of strength ε and observing, at the same periodic frequency, a modulation of strength A_1. The gain factor is defined as $\hat{G}(\omega) = A_1/\varepsilon$. With the above arguments the gain factor is (Richardson, 2007)

$$\hat{G}(\omega) = \frac{a_1}{\varepsilon} = -\frac{a_2}{\varepsilon}\,\frac{J_1^{\varepsilon}(u_{\rm low})}{J_1^{\rm free}(u_{\rm low})}\,. \tag{13.55}$$

The gain factor $\hat{G}(\omega)$ has an amplitude $|\hat{G}(\omega)|$ and a phase ϕ_G. Amplitude and phase of the gain factor of a population of exponential integrate-and-fire neurons are plotted in Fig. 13.9a.

The same numerical integration scheme that starts at the numerical threshold $\theta_{\rm reset}$ and integrates downward with appropriate initial conditions can also be applied to other, linear as well as nonlinear, neuron models. Furthermore, with the same scheme it is also possible to calculate the gain factor G_σ in response to a modulation of the variance $\sigma^2(t)$ (Fig. 13.9b), or the response G_ϑ to periodic modulation of model parameters such as the rheobase threshold $\vartheta_{\rm rh}$ (Richardson, 2007). For earlier results on G_σ see also Brunel and Hakim (1999), Lindner and Schimansky-Geier (2001) and Silberberg *et al*. (2004).

13.6 Neuronal adaptation and synaptic conductance

In the previous section we analyzed a population of exponential integrate-and-fire neurons driven by diffusive noise with mean $\mu(t)$ and strength $\sigma(t)$. At first glance, the results might seem of limited relevance and several concerns may be raised.

(i) What happens if we replace the one-dimensional exponential integrate-and-fire model by a neuron model with adaptation?

(ii) What happens if neurons are embedded into a network with coupling within and between several populations?

(iii) What happens if neurons don't receive synaptic current pulses that lead to a jump of the membrane potential but rather, more realistically, conductance-based input?

(iv) What happens if the input noise is not "white" but colored?

All of these questions can be answered and will be answered in this section. In fact, all questions relate to the same, bigger picture: suppose we would like to simulate a large network consisting of K populations. In each population, neurons are described by a multi-dimensional integrate-and-fire model, similar to the adaptive integrate-and-fire models of Chapter 6.

The set of equations (6.1) and (6.2) that controls the dynamics of a single neuron i is repeated here for convenience

$$\tau_m \frac{{\rm d}u_i}{{\rm d}t} = f(u_i) - R\sum_k w_{k,i} + RI_i(t), \tag{13.56}$$

$$\tau_k \frac{{\rm d}w_{k,i}}{{\rm d}t} = a_k\,(u - u_{\rm rest}) - w_{k,i} + b_k\tau_k \sum_{t^f} \delta(t - t_i^f)\,, \tag{13.57}$$

https://doi.org/10.1017/CBO9781107447615.016 Published online by Cambridge University Press

where $f(u) = -(u - u_{\rm rest}) + \Delta_T \exp[(u - \vartheta_{\rm rh})/\Delta_T]$ is the nonlinear spike generation mechanism of the exponential integrate-and-fire model. The voltage equation (13.56) is complemented by a set of adaptation variables $w_{k,i}$ which are coupled to the voltage and the spike firing via Eq. (13.57). The first of the above questions concerns the treatment of these slow adaptation variables in the Fokker–Planck framework.

In a network with a more realistic synapse model, the input current I_i of neuron i is generated as a conductance change, caused by the spike firings of other neurons j

$$I_i(t) = \sum_j \sum_f g_{ij}(t - t_j^f)\,(u_i - E_{ij}^{\rm syn})\,, \tag{13.58}$$

where $g_{ij}(s)$ for $s > 0$ describes the time course of the conductance change and $E_{ij}^{\rm syn}$ is the reversal potential of the synapse from j to i. Question (ii) concerns the fact that the spike firings are generated by the network dynamics, rather than by a Poisson process. Questions (iii) and (iv) focus on the aspects of conductance (rather than current) input and temporal extension of the conductance pulses.

Let us now discuss each of the four points in turn.

13.6.1 Adaptation currents

To keep the treatment simple, we consider the adaptive exponential integrate-and-fire model (AdEx) with a single adaptation current (see Eq. (6.3)). We drop the neuron index i, and consider, just as in the previous sections, that the stochastic spike arrival can be modeled by a mean $\mu(t) = R\,\langle I(t)\rangle$ plus a white-noise term ξ

$$\tau_m \frac{{\rm d}u}{{\rm d}t} = -(u - u_{\rm rest}) + \Delta_T \exp\left(\frac{u - \vartheta_{\rm rh}}{\Delta_T}\right) - R\,w + \mu(t) + \xi(t), \tag{13.59}$$

$$\tau_w \frac{{\rm d}w}{{\rm d}t} = a\,(u - u_{\rm rest}) - w + b\tau_w \sum_{t^f} \delta(t - t^f). \tag{13.60}$$

The stochastic input drives the neuron into a regime where the voltage fluctuates and the neuron occasionally emits a spike. Let us now assume that the input is stationary, i.e., the mean and variance of the input are constant. Suppose furthermore that the time constant τ_w of the adaptation variable w is larger than the membrane time constant and that the increase of w during spike firing is small: $b \ll 1$. In this case, the fluctuations of the adaptation variable w around its mean value $\langle w\rangle$ are small. Therefore, for the solution of the membrane potential density equations $p_0(u)$ the adaptation variable can be approximated by a constant $w_0 = \langle w\rangle$ (Richardson *et al.*, 2003; Gigante *et al.*, 2007). This separation-of-time-scales approach can also be extended to calculate the steady-state rate and time-dependent response for neurons with biophysically detailed voltage-gated currents (Richardson, 2009).

13.6.2 Embedding in a network

Embedding the model neurons into a network consisting of several populations proceeds along the same line of argument as in Section 13.4 or Chapter 12.

https://doi.org/10.1017/CBO9781107447615.016 Published online by Cambridge University Press

The mean input $\mu(t)$ to neuron i arriving at time t from population k is proportional to its activity $A_k(t)$. Similarly, the contribution of population k to the variance σ^2 of the input to neuron i is also proportional to $A_k(t)$; see Eq. (13.31). The stationary states and their stability in a network of adaptive model neurons can therefore be analyzed as follows.

(i) Determine the stationary state A_0 self-consistently. To do so, we use the gain function $g_\sigma(I_0)$ for our neuron model of choice, where the mean current $I_0 = \mu/R$ and the noise level σ depend on the activity A_0. The gain function $g_\sigma(I_0)$ of adaptive nonlinear integrate-and-fire neurons can be found using the methods discussed above.

(ii) Determine the response to periodic modulation of input current and input variance, $\hat{G}_\mu(\omega)$ and $\hat{G}_\sigma(\omega)$, respectively, using the methods discussed above.

(iii) Use the inverse Fourier transform to find the linear response filters $G_\mu(s)$ and $G_\sigma(s)$ that describes the population activity with respect to small perturbations of the input current $\Delta I(t)$ and to small perturbations in the noise amplitude $\sigma(t)$

$$A(t) = A_0 + \int_0^\infty G_\mu(s)\,\Delta I(t-s)\,\mathrm{d}s + \int_0^\infty G_\sigma(s)\,\Delta\sigma(t-s)\,\mathrm{d}s\,. \tag{13.61}$$

(iv) Exploit the fact that the current $I(t)$ and its fluctuations $\sigma(t)$ in a network with self-coupling, Eq. (13.31), are proportional to the current activity $A(t)$. If we set $\Delta A(t) = A(t) - A_0(t)$ we therefore have for the case of a single population feeding its activity back to itself

$$\Delta A(t) = \int_0^\infty [J_\mu\, G_\mu(s) + J_\sigma\, G_\sigma(s)]\,\Delta A(t-s)\,\mathrm{d}s, \tag{13.62}$$

where the constants J_μ and J_σ depend on the coupling parameters.

(v) Search for solutions $\Delta A(t) = \varepsilon \exp[\lambda(\omega)t]\cos(\omega t)$. The stationary state of asynchronous firing with activity A_0 is unstable if there exists a frequency for which $\lambda(\omega) > 0$.

The arguments in steps (i) to (v) do not rely on the assumption of current-based synapses. In fact, as we shall see now, conductance-based synapses can be, in the stationary state, well approximated by an equivalent current-based scheme.

13.6.3 Conductance input vs. current input

Throughout this chapter we assumed that spike firing by a presynaptic neuron j at time t_j^f generates in the postsynaptic neuron i an excitatory or inhibitory postsynaptic *current* pulse $w_{ij}\,\delta(t - t_j^f)$. However, synaptic input is more accurately described as a change in conductance $g(t - t_j^f)$, rather than as current injection (Destexhe *et al.*, 2003). As mentioned in Eq. (13.58), a time-dependent synaptic conductance leads to a total synaptic current into neuron i

$$I_i(t) = \sum_j \sum_f w_{ij} g_{ij}(t - t_j^f)\,(u_i(t) - E_{\mathrm{syn}}), \tag{13.63}$$

which depends on the momentary difference between the reversal potential E_{syn} and the membrane potential $u_i(t)$ of the postsynaptic neuron. A spike fired by a presynaptic neuron

https://doi.org/10.1017/CBO9781107447615.016 Published online by Cambridge University Press

j at time t_j^f can therefore have a bigger or smaller effect, depending on the state of the postsynaptic neuron; see Chapter 3.

Nevertheless we will now show that, in the state of stationary asynchronous activity, conductance-based input can be approximated by an effective current input (Lansky and Lanska, 1987; Richardson, 2004; Richardson and Gerstner, 2005; Wolff and Lindner, 2011). The main effect of conductance-based input is that the membrane time constant of the stochastically driven neuron is shorter than the "raw" passive membrane time constant (Bernander *et al.*, 1991; Destexhe *et al.*, 2003).

To keep the arguments transparent, we consider $N_{\rm E}$ excitatory and $N_{\rm I}$ inhibitory leaky integrate-and-fire neurons in the subthreshold regime

$$C\frac{{\rm d}u}{{\rm d}t} = -g_L\,(u-E_L) - g_E(t)\,(u-E_E) - g_I(t)\,(u-E_I), \tag{13.64}$$

where C is the membrane capacity, g_L the leak conductance and E_L, E_E, E_I are the reversal potentials for leak, excitation, and inhibition, respectively. We assume that input spikes at excitatory synapses lead to an increased conductance

$$g_E(t) = \Delta g_E \sum_j \sum_f \exp[-(t-t_j^f)/\tau_E]\Theta(t-t_j^f) \tag{13.65}$$

with amplitude Δg_E and decay time constant τ_E. The Heaviside step function Θ assures causality in time. The sum over j runs over all excitatory synapses. Input spikes at inhibitory synapses have a similar effect, but with jump amplitude Δg_I and decay time constant τ_I. We assume that excitatory and inhibitory input spikes arrive with a total rate ν_E and ν_I, respectively. For example, in a population of excitatory and inhibitory neurons the total excitatory rate to neuron i would be the number of excitatory presynaptic partners C_E of neuron i times the typical firing rate of a single excitatory neuron.

Using the methods from Chapter 8 we can calculate the mean excitatory conductance

$$g_{E,0} = \Delta g_E\, \nu_E\, \tau_E\,, \tag{13.66}$$

where ν_E is the total spike arrival rate at excitatory synapses, and analogously for the mean inhibitory conductance. The variance of the conductance is

$$\sigma_E^2 = 0.5(\Delta g_E)^2\, \nu_E\, \tau_E. \tag{13.67}$$

The mathematical analysis of conductance input proceeds in two steps. First, we write the conductance as the mean $g_{E,0}$ plus a fluctuating component $g_{E,f}(t) = g_E(t) - g_{E,0}$. This turns Eq. (13.64) into a new equation

$$C\frac{{\rm d}u}{{\rm d}t} = -g_0\,(u-\mu) - g_{E,f}(t)\,(u-E_E) - g_{I,f}(t),(u-E_I), \tag{13.68}$$

with a total conductance $g_0 = g_L + g_{E,0} + g_{I,0}$ and an input-dependent equilibrium potential

$$\mu = \frac{g_L E_L + g_{E,0} E_E + g_{I,0} E_I}{g_0}\,. \tag{13.69}$$

We emphasize that Eq. (13.68) looks just like the original equation (13.64). The major differences are, however, that the dynamics in Eq. (13.64) is characterized by a raw

https://doi.org/10.1017/CBO9781107447615.016 Published online by Cambridge University Press

membrane time constant C/g_L whereas Eq. (13.68) is controlled by an *effective* membrane time constant

$$\tau_{\rm eff} = \frac{C}{g_0} = \frac{C}{g_L + g_{E,0} + g_{I,0}}, \tag{13.70}$$

and a mean depolarization μ which acts as an effective equilibrium potential (Johannesma, 1968).

In the second step we compare the momentary voltage $u(t)$ with the effective equilibrium potential μ. The fluctuating part of the conductance in Eq. (13.68) can therefore be written as

$$g_{E,f}(t)\,(u - E_E) = g_{E,f}(t)\,(\mu - E_E) + g_{E,f}(t)\,(u - \mu), \tag{13.71}$$

and similarly for the inhibitory conductance. The second term on the right-hand side of Eq. (13.71) is small compared to the first term and needs to be dropped to arrive at a consistent diffusion approximation (Richardson and Gerstner, 2005). The first term on the right-hand side of Eq. (13.71) does not depend on the membrane potential and can therefore be interpreted as the summed effects of postsynaptic *current* pulses. Thus, in the stationary state, a conductance-based synapse model is well approximated by a current-based model of synaptic input. However, we need to use the *effective* membrane time constant $\tau_{\rm eff}$ introduced above in Eq. (13.70) in the voltage equation.

Example: Response to conductance-modulating input

Suppose we have a population of uncoupled exponential integrate-and-fire neurons. Using the methods discussed above in Section 13.5, we can calculate the linear response $G(s)$ of the population to a short conductance pulse $g_E(t)$ at an excitatory synapse (Fig. 13.10). The response to some arbitrary time-dependent conductance input can then be predicted by convolving the conductance change with the filter response. The Fourier transform of the filter predicts the response to sinusoidal conductance modulation with period T (Fig. 13.10).

13.6.4 Colored noise (*)

In the previous subsection, we replaced synaptic conductance pulses by current input. If the time constants $\tau_{\rm E}$ and $\tau_{\rm I}$ of excitatory and inhibitory synapses are sufficiently short, we may approximate stochastic spike arrivals by white noise. Some synapse types, such as the NMDA component of excitatory synapses, are, however, rather slow (see Chapter 3). As a result of this, a spike that has arrived at an NMDA synapse at time t_0 generates a fluctuation of the input current that persists for tens of milliseconds. Thus the fluctuations in the input exhibit temporal correlations, a situation that is termed colored noise, as opposed to white noise; see Chapter 8. Colored noise represents the temporal smoothing caused by slow synapses in a compact form.

https://doi.org/10.1017/CBO9781107447615.016 Published online by Cambridge University Press

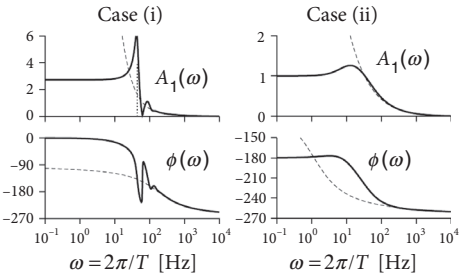

Fig. 13.10 Conductance input. Frequency response of the population of exponential integrate-and-fire neurons as in Fig. 13.9, but to conductance modulation. For high frequencies, the phase slowly approaches a lag of 270° which can be interpreted as a phase advance of 90°. Solid line: numerical solution. Dashed line: analytical high-frequency response; cases (i) and (ii) correspond to low noise and high noise, respectively. Adapted from Richardson (2007).

There are two different approaches to colored noise in the membrane potential density equations.

The first approach is to approximate colored noise by white noise and replace the temporal smoothing by a broad distribution of delays. To keep the treatment transparent, let us assume a current-based description of synaptic input. The mean input to a neuron i in population n arising from other populations k is

$$I_i(t) = \sum_k C_{nk} w_{nk} \int_0^\infty \alpha_{nk}(s) A_k(t-s)\,\mathrm{d}s\,, \tag{13.72}$$

where C_{nk} is the number of presynaptic partner neurons in population k, w_{nk} is the typical weight of a connection from k to a neuron in population n and $\alpha_{nk}(s)$ is the time course of a synaptic current pulse caused by a spike fired in population k at $s = 0$. Suppose C_{nk} is a large number, say $C_{nk} = 1000$, but the population k itself is at least 10 times larger (e.g., $N_k = 10\,000$) so that the connectivity $C_{nk}/N_k \ll 1$. We now replace the broad current pulses $\alpha(s)$ by short pulses $q\,\delta(s-\Delta)$ where δ denotes the Dirac δ-function and $q = \int_0^\infty \alpha(s)\,\mathrm{d}s$ and $\Delta > 0$ is a transmission delay. For each of the C_{nk} connections we randomly draw the delay Δ from a distribution $p(\Delta) = \alpha(\Delta)/q$. Because of the low connectivity, we may assume that the firing of different neurons is uncorrelated. The mean input current $I_i(t)$ to neuron i is then given again by Eq. (13.72), with fluctuations around the mean that are approximately white, because each spike arrival causes only a momentary current pulse. The broad distribution of delays stabilizes the stationary state of asynchronous firing (Brunel, 2000).

The second approach consists in an explicit model of the synaptic current variables. To keep the treatment transparent and minimize the number of indices, we focus on a single population coupled to itself and suppose that the synaptic current pulses are exponential $\alpha(s) = (q/\tau_q)\exp(-s/\tau_q)$. The driving current of a neuron i in a population n arising from

https://doi.org/10.1017/CBO9781107447615.016 Published online by Cambridge University Press

spikes of the same population is then described by the differential equation

$$\frac{\mathrm{d}I_i}{\mathrm{d}t} = -\frac{I_i}{\tau_q} + C_{nn} w_{nn} \frac{q}{\tau_q} A_n(t), \tag{13.73}$$

which we can verify by taking the temporal derivative of Eq. (13.72). As before the population activity $A_n(t)$ can be decomposed into a mean $\mu(t)$ (which is the same for all neurons) and a fluctuating part $\xi_i(t)$ with white-noise characteristics:

$$\frac{\mathrm{d}I_i}{\mathrm{d}t} = -\frac{I_i}{\tau_q} + \mu(t) + \xi_i(t)\,. \tag{13.74}$$

However, Eq. (13.74) does not lead directly to spike firing but needs to be combined with the differential equation for the voltage

$$\tau_m \frac{\mathrm{d}u_i}{\mathrm{d}t} = f(u_i) + R I_i(t)\,, \tag{13.75}$$

and the reset condition: if $u = \theta_{\mathrm{reset}}$ then $u = u_r$. Since we now have two coupled differential equations, the momentary state of a population of N neurons is described by a two-dimensional density $p(u,I)$.

We recall that, in the case of white noise, the membrane potential density at threshold vanishes. The main insight for the mathematical treatment of the membrane potential density equations in two dimensions is that the density at threshold $p(\theta_{\mathrm{reset}}, I(t))$ is finite, whenever the momentary slope of the voltage $\mathrm{d}u/\mathrm{d}t \propto RI(t) + f(\theta_{\mathrm{reset}})$ is positive (Fourcaud and Brunel, 2002).

13.7 Summary

The momentary state of a population of one-dimensional integrate-and-and fire neurons can be characterized by the membrane potential density $p(u,t)$. The continuity equation describes the evolution of $p(u,t)$ over time. In the special case that neurons in the population receive many inputs that each cause a small change of the membrane potential, the continuity equation has the form of a Fokker–Planck equation. Several populations of integrate-and-fire neurons interact via the population activity $A(t)$, which is identified with the flux across the threshold.

The stationary state of the Fokker–Planck equation and the stability of the stationary solution can be calculated by a mix of analytical and numerical methods, be it for a population of independent or interconnected neurons. The mathematical and numerical methods developed for membrane potential density equations apply to leaky as well as to arbitrary nonlinear one-dimensional integrate-and-fire models. A slow adaptation variable such as in the adaptive exponential integrate-and-fire model can be treated as quasi-stationary in the proximity of the stationary solution. Conductance input can be approximated by an equivalent current-based model.

Literature

The formulation of the dynamics of a population of integrate-and-fire neurons on the level of membrane potential densities has been developed by Abbott and van Vreeswijk (1993), Brunel and Hakim (1999), Fusi and Mattia (1999), Nykamp and Tranchina (2000), Omurtag *et al*. (2000), and Knight (2000), but the Fokker–Planck equation has been used much earlier for the probabilistic description of a single neuron driven by stochastic spike arrivals (Johannesma, 1968; Capocelli and Ricciardi, 1971; Ricciardi, 1976). The classic application of the Fokker–Planck approach to a network of excitatory and inhibitory leaky integrate-and-fire neurons is Brunel (2000). For the general theory of Fokker–Planck equations see Risken (1984).

Efficient numerical solutions of the Fokker–Planck equation, for both stationary input and periodic input, have been developed by M. J. E. Richardson (2007, 2009). These methods can be used to find activity in networks of nonlinear integrate-and-fire models, and also of generalized neuron models with slow spike-triggered currents or conductances (Richardson, 2009). For the treatment of colored noise, see Fourcaud and Brunel (2002).

Exercises

1. **Diffusion limit in the quadratic integrate-and-fire model**. *Consider a population of quadratic integrate-and-fire models. Assume that spikes from external sources arrive at excitatory and inhibitory synapses stochastically, and independently for different neurons, at a rate $\nu_E(t)$ and $\nu_I(t)$, respectively.*

   (a) Write down the membrane potential density equations assuming that each spike causes a voltage jump by an amount $\pm\Delta u$.

   (b) Take the diffusion limit so as to arrive at a Fokker–Planck equation.
2. **Voltage distribution of the quadratic integrate-and-fire model**. *Find the stationary solution of the membrane potential distribution for the quadratic integrate-and-fire model with white diffusive noise.*
3. **Non-leaky integrate-and-fire model.** *Consider a non-leaky integrate-and-fire model subject to stochastic spike arrival*

$$\frac{\mathrm{d}u}{\mathrm{d}t} = \frac{1}{C} I(t) = \frac{q}{C} \sum_f \delta(t - t^f), \tag{13.76}$$

   where q is the charge that each spike puts on the membrane and the spike arrival rate is constant and equal to ν. At $u = \vartheta = 1$ the membrane potential is reset to $u = u_r = 0$.

   (a) Formulate the continuity equation for the membrane potential density equation.

   (b) Make the diffusion approximation.

   (c) Solve for the stationary membrane potential density distribution under the assumption that the flux through u_r vanishes.
4. **Linear response.** *A population is driven by a current $I_0 + I_1(t)$. The response of the population is described by*

$$A(t) = A_0 + A_1(t) = A_0 + \int_0^\infty G(s)\, I_1(t-s)\, \mathrm{d}s, \tag{13.77}$$

   where G is called the linear response filter.

https://doi.org/10.1017/CBO9781107447615.016 Published online by Cambridge University Press

(a) Take the Fourier transformation and show that the convolution with the filter G turns into a simple multiplication:

$$\hat{A}_1(\omega) = \hat{G}(\omega)\,\hat{I}_1(\omega), \tag{13.78}$$

where the hats denote the Fourier transformed variable.

Hint: Replace $G(s)$ in Eq. (13.77) *by a causal filter $G_c(s) = 0$ for $s \le 0$ and $G_c(s) = G(s)$ for $s > 0$, extend the lower integral bound to $-\infty$, and apply standard rules for Fourier transforms.*

(b) The squared quantity $|\hat{I}_1(\omega)|^2$ is the power of the input at frequency ω. What is the power $|\hat{A}_1(\omega)|^2$ of the population activity at frequency ω?

(c) Assume that the filter is given by $G(s) = \exp[-(s-\Delta)/\tau_g]$ for $s > \Delta$ and zero otherwise. Calculate $\hat{G}(\omega)$.

(d) Assume that the input current has a power spectrum $|\hat{I}_1(\omega)|^2 = (c/\omega)$ with $c > 0$ for $\omega > \omega_0$ and zero otherwise.

What is the power spectrum of the population activity with a linear filter as in (iii)?

5. **Stability of stationary state**. *The response of the population is described by*

$$A(t) = A_0 + A_1(t) = A_0 + \int_0^\infty G(s)\,I_1(t-s)\,\mathrm{d}s, \tag{13.79}$$

where G is the linear response filter. Set $G(s) = \exp[-(s-\Delta_g)/\tau_g]$ for $s > \Delta_g$ and zero otherwise.

Assume that the input arises due to self-coupling with the population:

$$I_1(t) = \int_0^\infty \alpha(s)\,A_1(t-s)\,\mathrm{d}s\,. \tag{13.80}$$

Set $\alpha(s) = (\alpha_0/\tau_\alpha)\exp[-(s-\Delta_\alpha)/\tau_\alpha]$ for $s > \Delta_\alpha$ and zero otherwise.

(a) Search for solutions $A_1(t) \propto \exp[\lambda(\omega)t]\cos(\omega t)$. The stationary state A_0 is stable if $\lambda < 0$ for all frequencies ω.

(b) Analyze the critical solutions $\lambda = 0$ as a function of the delays Δ_G and Δ_α and the feedback strength α_0.

6. **Conductance input**. *Consider N_E excitatory and N_I inhibitory leaky integrate-and-fire neurons in the subthreshold regime*

$$C\frac{\mathrm{d}u}{\mathrm{d}t} = -g_L\,(u-E_L) - g_E(t)\,(u-E_E) - g_I(t)\,(u-E_I), \tag{13.81}$$

where C is the membrane capacity, g_L the leak conductance and E_L, E_E, E_I are the reversal potentials for leak, excitation, and inhibition, respectively. Assume that input spikes at excitatory arrive at a rate ν_E and lead to a conductance change

$$g_E(t) = \Delta g_E \sum_j \sum_f \exp[-(t-t_j^f)/\tau_E] \quad \text{for } t > t_j^f \tag{13.82}$$

(and zero otherwise) with amplitude Δg_E and decay time constant τ_E. A similar expression holds for inhibition with $\Delta g_I = 2\Delta g_E$ and $\tau_I = \tau_E/2$. Spike arrival rates are identical $\nu_I = \nu_E$.

(a) Determine the mean potential μ.

(b) Introduce

$$\alpha_E(t-t_j^f) = a_E\,\exp[-(t-t_j^f)/\tau_E]\Theta(t-t_j^f)\,(\mu - E_E) \tag{13.83}$$

and an analogous expression for inhibitory input currents α_I.

Show that the membrane with conductance-based synapses Eq. (13.81) *can be approximated by a model with* current-based *synapses*

$$\tau_\mathrm{eff}\frac{\mathrm{d}u}{\mathrm{d}t} = -(u-E_L) + \sum_{j\in N_E}\sum_f \alpha_E(t-t_j^f) + \sum_{j\in N_I}\sum_f \alpha_I(t-t_j^f), \tag{13.84}$$

https://doi.org/10.1017/CBO9781107447615.016 Published online by Cambridge University Press

where E_L is the leak potential defined earlier in Eq. (13.81). *Determine a_E, a_I and τ_{eff}. What are the terms that are neglected in this approximation? Why are they small?*

(c) Assume that the reversal potential for inhibition and leak are the same $E_I = E_L$. What is the mean potential μ in this case? How does inhibitory input manifest itself? What would change if you replaced inhibition by a constant current that sets the mean membrane potential (in the presence of the same amount of excitation as before) to μ?

7. **Firing rate of leaky integrate-and-fire neurons in the Brunel–Hakim formulation**.

Show that the Siegert formula of Eq. (13.30) can be also written in the form (Brunel and Hakim, 1999)

$$\frac{1}{A_0\,\tau_m} = 2\int_0^\infty \mathrm{d}u\,\mathrm{e}^{-u^2}\left[\frac{\mathrm{e}^{2y_2u} - \mathrm{e}^{2y_1u}}{u}\right] \tag{13.85}$$

with $y_2 = (\vartheta - h_0)/\sigma$ and $y_1 = (u_r - h_0)/\sigma$.

Hint: Use the definition of the error function erf *given above Eq.* (13.30).

https://doi.org/10.1017/CBO9781107447615.016 Published online by Cambridge University Press